

Periodic boundary conditions

Farhang Radjai and Charles Voivret

*Laboratoire de Mécanique et Génie Civil, CNRS - Université Montpellier 2, Place
Eugène Bataillon, 34095 Montpellier cedex 05*

1 Introduction

The discrete-element approach is a key research tool for granular materials. Given an appropriate model of the material in terms of particle shapes and size distributions, mechanical properties and their interaction laws, the mechanical behavior (rheology) is a consequence of the collective dynamics of the particles simulated by a discrete element method (DEM). Such simulations give access not only to the macro-scale response to external loading but provide also detailed information on the microstructure and its evolution. However, the emerging behavior is all the more intrinsic to the material and devoid of spurious effects as the numerical sample is homogeneous and large in the number of particles. This corresponds to a *homogeneous behavior* of a representative volume element (RVE) of the material. Note that since granular materials are characterized by a highly inhomogeneous microstructure and dynamics at the particle scale, the homogeneity of a volume element should be described in terms of the statistical representativity of micro-scale variables.

In practice, the number of particles is limited (below 10^5 for month-long simulations) by the available computation power and memory and thus the conditions of homogeneity and representativity are not always fulfilled. Let us consider, for example, a dense 3D sample of $50 \times 50 \times 50$ mono-sized particles confined in a cubic box. In this system, the mono-layer covering the internal walls of the box contains $\sim 12\%$ of particles. The packing fraction is generally lower in the neighborhood of rigid walls and the wall-induced order propagates into the bulk. Moreover, the distortion of the box by simple shearing gives rise to strong arching effect at the corners of the box, generating thus stress gradients over long distances inside the sample Thornton and Zhang [2001]. Such effects arise also in experimental tests on granular materials, but the number of particles in experiments is generally much higher. The wall effects are more critical in numerical simulations mainly as a result of the low number of particles.

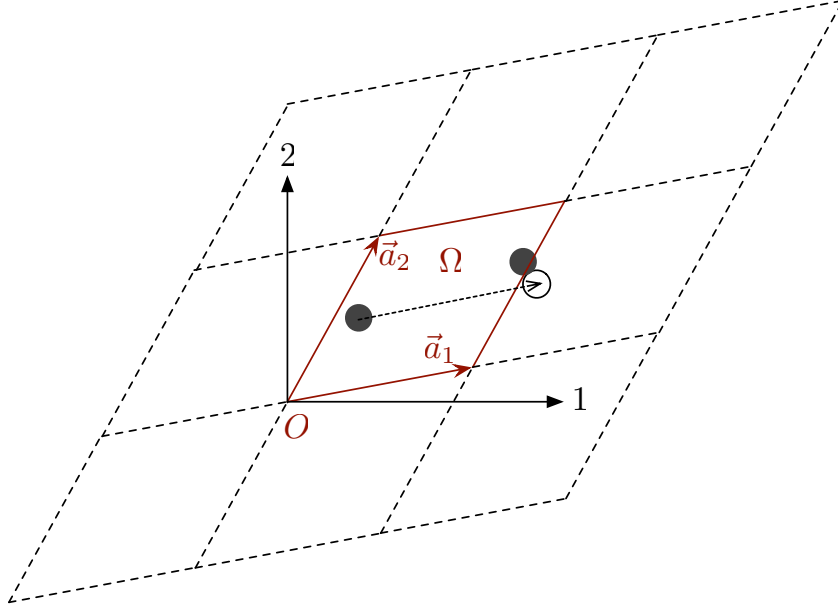


Fig. 1. A two-dimensional simulation cell Ω with its basis vectors in an absolute frame. A particle located at the right boundary interacts with the image of another particle located at the left boundary.

The undesired effects of wall boundaries can be eliminated by means of periodic boundary conditions. In this framework, the simulation domain becomes a unit cell containing the particles with periodic copies paving the whole space. The particles located at the borders of the simulation cell may then interact with the image particles in a neighboring cell; figure 1. In this way, the periodic boundary conditions extend the system boundaries to the infinity so that the simulation cell simply plays the role of a coordinate system to locate particle positions Allen and Tildesley [1987]. The origin of the coordinates being immaterial, the dynamics of the particles is invariant by translation and therefore necessarily homogeneous.

With wall boundaries, the external stresses or displacements are applied on the simulation box through wall degrees of freedom which are alternatively kept free or frozen depending on whether a stress or a displacement is monitored in a given space direction. With periodic boundary conditions, this role is played by the collective degrees of freedom carried by the coordinate system, whose basis vectors become dynamic variables, and their conjugate stresses expressed as a state function of the granular configuration. This approach was first formulated by Parrinello and Rahman by assuming a Hamiltonian conservative system Parrinello and Rahman [1980]. With this formalism, the particles can be subjected to arbitrary homogeneous loadings. The simulation cell evolves with the particles and may change its shape and volume.

We present here a method for the prescription of periodic boundary conditions in DEM simulations of granular materials. This method is similar in

practice to that of Parrinello and Rahman, but since the particle interactions are dissipative in a granular system, the equations of motion for collective dynamic variables can not be based on a Hamiltonian. We consider in detail the particular kinematics of periodic systems, the equations of dynamics and time-stepping schemes for MD-DEM and CD-DEM.

2 Kinematics

2.1 Periodicity in position

Let us consider a collection of N_p particles with their centers contained in a cell Ω of volume V . The cell can have any shape allowing for a periodic tessellation of space. The simplest shape is a parallelepiped (triclinic) in 3D or a parallelogram in 2D. Other shapes such as rhombic dodecahedron in 3D and hexagon in 2D are equally possible Allen and Tildesley [1987]. The cell Ω and its replicas define a regular lattice characterized by its basis vectors $(\vec{a}_1, \vec{a}_2, \vec{a}_3)$. In the case of a parallelepiped, the basis vectors may simply be the three sides of the parallelepiped; figure 1. The origin O of the simulation cell is a vertex of the cell of coordinates $(0, 0, 0)$ and its replicas are defined by three indices (i_1, i_2, i_3) corresponding to a translation of the origin by the vector $i_1 \vec{a}_1 + i_2 \vec{a}_2 + i_3 \vec{a}_3$. Then, the coordinates $\vec{r}(i')$ of the image i' of a particle $i \in \Omega$ of coordinates $\vec{r}(i)$ are given by:

$$\vec{r}(i') = \vec{r}(i) + \sum_{k=1}^3 i_k \vec{a}_k \quad (1)$$

The particles belonging to the cell Ω , characterized by $i_1 = i_2 = i_3 = 0$, can interact with the particles of the same cell but also with image particles in the neighboring cells characterized by $i_k \in \{-1, 0, 1\}$. There are $3^D - 1$ cells surrounding the simulation cell and they are involved in the search of contact partners for each particle. The distance between two particles i et $j \in \Omega$ is the shortest distance separating i from j or from one of its images j' . As the system evolves in time, a particle i may leave Ω but one of its images i' enters Ω at the same moment. In order to keep all original particles in the cell Ω , the status ‘‘original’’ should be reserved to the particles whose centers belong to Ω . Hence, whenever a particle i leaves the simulation cell, it becomes an image of i' which then becomes original. This means that, a particle crossing a border of the simulation cell, returns to the cell by crossing another border.

2.2 Reduced coordinates

The particle positions can be represented in terms of the basis vectors $\{\vec{a}_k\}$:

$$\vec{r}(i) = \sum_{k=1}^3 s_k(i) \vec{a}_k = \mathbf{h} \vec{s}(i) \quad (2)$$

The components of $\vec{s}(i)$ define the *reduced coordinates* of particle i . For the original particles, these coordinates range from 0 to 1, corresponding thus to a point in a unitary cube. The matrix \mathbf{h} transforms reduced coordinates $\vec{s}(i)$ into absolute coordinates $\vec{r}(i)$. The three columns of \mathbf{h} are simply the three components of the basis vectors: $h_{kl} = (a_l)_k$.

Equation (2) shows that the position vector $\vec{r}(i)$ of a particle i can change either as a result of the variation of basis vectors $\{\vec{a}_k\}$ or due to the evolution of reduced coordinates $s_k(i)$. In the first case the variation is homogeneous as it affects the positions of all particles in the cell whereas the second case affects only the particle i . To distinguish these two contributions, we differentiate equation (2) with respect to time:

$$\dot{\vec{r}}(i) = \dot{\mathbf{h}} \vec{s}(i) + \mathbf{h} \dot{\vec{s}}(i) \equiv \vec{u}(i) + \vec{v}(i) \quad (3)$$

The affine velocity field $\vec{u}(i) \equiv \dot{\mathbf{h}} \vec{s}(i)$ represents a homogeneous deformation of the whole set of particles. On the contrary, the velocity field $\vec{v}(i) \equiv \mathbf{h} \dot{\vec{s}}(i)$ is non-affine and describes the proper (or fluctuating) velocities of the particles with respect to a background of homogeneous deformation. Since the homogeneous deformation is carried only by the field $\vec{u}(i)$, the average value of the fluctuating part $\vec{v}(i)$ must be zero. Hence, we have

$$\langle \dot{\vec{s}} \rangle = \frac{1}{N_p} \sum_{i=1}^{N_p} \dot{\vec{s}}(i) = 0 \quad (4)$$

The reduced coordinates can be used to manage the image particles. From the relations (2) and (1) one gets the following relation between the original reduced coordinates and their images:

$$s_k(i') = s_k(i) + i_k \quad (5)$$

Therefore, the reduced coordinates of the image particles in the neighboring cells are simply obtained by unit translations along the three space directions $k = 1, 2, 3$.

2.3 Periodicity in velocity

Driving equation (5) with respect to time, we see that the reduced velocities are periodic:

$$\dot{s}_k(i') = \dot{s}_k(i) \quad (6)$$

As a consequence, the no-affine velocities are strictly periodic:

$$\vec{v}(i') = \mathbf{h} \dot{\vec{s}}(i') = \mathbf{h} \dot{\vec{s}}(i) = \vec{v}(i) \quad (7)$$

By definition, the affine velocities are non-periodic. Indeed, we have

$$u_k(i') = \sum_l \dot{h}_{kl} s_l(i') = \sum_l \dot{h}_{kl} (s_l(i) + i_l) = u_k(i) + \sum_l \dot{h}_{kl} i_l \quad (8)$$

For the calculation of relative velocities at the contact point between an original particle and an image particle, one should thus take this affine transformation of the velocities into account.

The velocity gradient tensor $\dot{\mathbf{L}}$ in the simulation cell Ω derives from the affine field $\vec{u}(i)$. By definition, we have

$$\vec{u}(i) = \dot{\mathbf{h}} \vec{s}(i) \equiv \dot{\mathbf{L}} \vec{r}(i) = \dot{\mathbf{L}} \mathbf{h} \vec{s}(i) \quad (9)$$

whence

$$\dot{\mathbf{L}} = \dot{\mathbf{h}} \mathbf{h}^{-1} \quad (10)$$

and the strain-rate tensor $\dot{\varepsilon}$ is the symmetric part of $\dot{\mathbf{L}}$ given by

$$\dot{\varepsilon} = \frac{1}{2}(\dot{\mathbf{L}} + \dot{\mathbf{L}}^T) \quad (11)$$

where $\dot{\mathbf{L}}^T$ represents the transpose of $\dot{\mathbf{L}}$.

The antisymmetric part $(\mathbf{L} - \mathbf{L}^T)/2$ corresponds to rigid rotations of the cell Ω and its replicas. However, these rotations are immaterial for a periodic system. Therefore, at least three elements (over nine) of the tensor $\dot{\mathbf{L}}$ should be fixed. For example, without losing generality in the deformations of the simulation cell, the basis vectors \vec{a}_1 and \vec{a}_2 can be forced to remain on the plane $z = 0$ and \vec{a}_3 on the plane $y = 0$, so that $h_{13} = h_{23} = h_{32} = 0$. Another solution consists

in canceling the antisymmetric part by imposing the velocity gradient tensor to be symmetric $\dot{\mathbf{L}} = \dot{\boldsymbol{\varepsilon}}$. This implies the symmetry of the matrix \mathbf{h} Nosé and Klein [1986, 1983].

2.4 Metric tensor

In addition to the particle degrees of freedom, a granular system with periodic boundary conditions has collective degrees of freedom represented by the matrix \mathbf{h} . We have seen that the strain-rate tensor $\dot{\boldsymbol{\varepsilon}}$ (as well as the cumulative deformation tensor $\boldsymbol{\varepsilon} = \int \dot{\boldsymbol{\varepsilon}} dt$) plays in practice the same role and can thus be used to represent the collective degrees of freedom. Another useful variable is the *metric tensor* \mathbf{g} defined by

$$\mathbf{g} \equiv \mathbf{h}^T \mathbf{h} \tag{12}$$

This tensor is symmetric and its diagonal elements describe the lengths of the three basis vectors whereas its off-diagonal elements describe the angles between those vectors Souza and Martins [1997].

The “metric” character of the tensor \mathbf{g} is related to the fact that the distance $|\vec{r}(i) - \vec{r}(j)|^2$ between two particles i et j is given by

$$|\vec{r}(i) - \vec{r}(j)|^2 = \{\vec{r}(i) - \vec{r}(j)\}^T \{\vec{r}(i) - \vec{r}(j)\} = \{\vec{s}(i) - \vec{s}(j)\}^T \mathbf{g} \{\vec{s}(i) - \vec{s}(j)\} \tag{13}$$

This means that the periodic system may be described by the reduced coordinates $\vec{s}(i)$ of the particles moving in a space with the metrics \mathbf{g} . This representation of the system is strictly equivalent to the representation in terms of absolute coordinates $\vec{r}(i)$ of the particles and the matrix \mathbf{h} considered as independent degrees of freedom. The matrix \mathbf{h} and the metric tensor \mathbf{g} change with the particle configuration according to the equations of dynamics, which will be discussed in section 3.

2.5 Modular transformations

For a given configuration $\{\vec{r}(i)\}$ of the particles with their images, the matrix \mathbf{h} allows us to define the reduced coordinates $\vec{s}(i) = \mathbf{h}^{-1} \vec{r}(i)$. But the definition of the simulation cell Ω , and thus that of \mathbf{h} , is not unique. One example is displayed in figure 2 where by moving a subset of particles $\in \Omega$ parallel to $-\vec{a}_1$, one obtains a new cell Ω' of the same volume as Ω and containing exactly one image of each particle. The replicas of the new cell Ω' tessellate the space as do

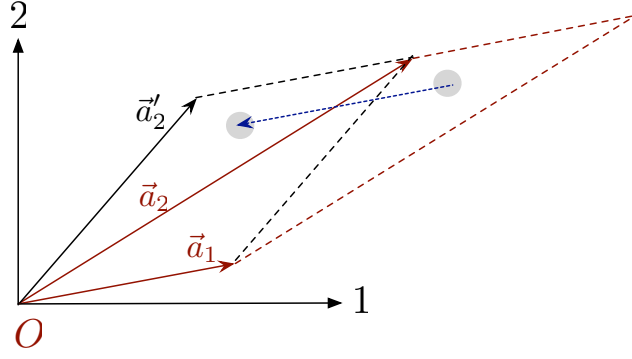


Fig. 2. Modular transformation of the cell defined by the vectors $\{\vec{a}_1, \vec{a}_2\}$ into another cell defined by the vectors $\{\vec{a}'_1 = \vec{a}_1, \vec{a}'_2 = \vec{a}_2 - \vec{a}_1\}$.

those of Ω . The basis vectors in this “modular” transformation change from $\{\vec{a}_1, \vec{a}_2\}$ to $\{\vec{a}_1, \vec{a}_2 - \vec{a}_1\}$.

The modular transformation, denoted by $\mathbf{T}_{\Omega'/\Omega}$, is linear:

$$\mathbf{h}' = \mathbf{T}_{\Omega'/\Omega} \mathbf{h} \quad (14)$$

The basis vectors of the matrix \mathbf{h} may be modified by \mathbf{T} in the course of simulation provided the velocities $\dot{\mathbf{h}}$ are modified, as well. In the example of figure 2, we change from the matrix $\mathbf{h} = \{\vec{a}_1, \vec{a}_2\}$ et $\dot{\mathbf{h}} = \{\dot{\vec{a}}_1, \dot{\vec{a}}_2\}$ to the matrices $\mathbf{h}' = \{\vec{a}_1, \vec{a}_2 - \vec{a}_1\}$ and $\dot{\mathbf{h}}' = \{\dot{\vec{a}}_1, \dot{\vec{a}}_2 - \dot{\vec{a}}_1\}$. These transformations should conserve the velocities $\vec{v}(i)$. It is therefore necessary to recalculate the reduced coordinates and their velocities for all particles: $\vec{s}'(i) = \mathbf{h}'^{-1} \vec{r}'(i)$ et $\dot{\vec{s}}'(i) = \mathbf{h}'^{-1} \vec{v}(i)$. The modular transformation may thus be seen as a re-definition of original particles.

The modular transformation can be used to separate the collective dynamic variables condensed in the matrix \mathbf{h} from the graphical representation of the simulation cell. In fact, \mathbf{h} represents at the same time the shape of the simulation cell and collective variables of the system. But an original particle is strictly equivalent to all its images so that the calculations can be performed with the matrix \mathbf{h} attributed to a cell Ω and the particles represented in another cell Ω' related to Ω by a modular transformation. For instance, let us assume that the initial cell Ω is a rectangular parallelepiped of basis vectors $\mathbf{h} = \{\vec{a}_1, \vec{a}_2, \vec{a}_3\}$. Incremental plane shearing of the system in the direction 1 transforms the cell into another parallelepiped Ω' of basis vectors $\mathbf{h}' = \{\vec{a}'_1, \vec{a}'_2, \vec{a}'_3\}$ defined by $\vec{a}'_3 = \vec{a}_3$, $\vec{a}'_1 = \alpha \vec{a}_1$, $\vec{a}'_2 = \nu \vec{a}_1 + \beta \vec{a}_2$, that corresponds to the elongations α and β along the directions 1 et 2, together with shearing β along the direction 1. Obviously, the deformed cell Ω' is the modular transform of a cell Ω'' characterized by $\mathbf{h}'' = \{\vec{a}''_1, \vec{a}''_2, \vec{a}''_3\}$ with $\vec{a}''_3 = \vec{a}_3$, $\vec{a}''_1 = \alpha \vec{a}_1$, $\vec{a}''_2 = \beta \vec{a}_2$. The particles can thus be represented in the rectangular box Ω'' by applying the modular transformation $\mathbf{T}_{\Omega''/\Omega'}$. In other words, the calculations

are performed with \mathbf{h} but the particles are represented in the rectangular cell Ω'' .

These boundary conditions for shearing are known as Lee-Edwards boundary conditions Allen and Tildesley [1987], Peyneau and Roux [2008a,b]. As we shall see in section 3, these limit conditions can be used alternatively with shear stress or shear strain imposed. In the same way, the cell dimensions can be fixed. In this case, considering the replicas of the simulation cell Ω'' , the Lees-Edwards conditions are equivalent to rigid displacements of the neighboring cells in the direction 2 at the rates $\dot{h}_{12}h_{22}$ and $-\dot{h}_{12}h_{22}$ on the opposite sides of the central cell. This representation has the advantage of keeping the shape of the simulation cell during shear. It should, however, be remarked that even strong distortions of the cell are not harmful for the calculations as, in contrast to wall boundaries, the particles located at the corners of the cell interact with image particles and may freely leave the cell.

3 Dynamics

In this section, we consider the equations of motion for the particles and collective degrees of freedom. The presented formalism is a generalization of that of Parrinello et Rahman to dissipative systems Parrinello and Rahman [1980]. We will introduce different writings of these equations that may turn out to be more or less adapted to the numerical method employed.

3.1 Collective degrees of freedom

Let us consider in the first place the collective degrees of freedom h_{kl} upon which depends the velocity-gradient tensor $\dot{\mathbf{L}}_{kl}$ and affine velocities $u_k(i) = \dot{h}_{kl}s_l(i)$. We assume that these variables are governed by the equations of dynamics:

$$m_h \ddot{h}_{kl} = F_{(h_{kl})} \quad (15)$$

where m_h is a fictive mass attributed to the collective variables and $F_{(h_{kl})}$ represents the “generalized force” associated with h_{kl} . These generalized forces are conjugate variables of h_{kl} in the sense that the rate \dot{W} of the work consumed by these forces is

$$\dot{W} = \sum_{kl} \dot{h}_{kl} \cdot F_{(h_{kl})} \quad (16)$$

In order to determine $F_{(h_{kl})}$, we may exploit the duality between the velocity-gradient tensor and stress tensor defined over the simulation cell. Since $\dot{\mathbf{L}}$ is an Eulerian tensor, its conjugate variable is the Cauchy stress tensor σ , which is also an Eulerian tensor. By definition, the power produced by the stresses per unit volume is the scalar product of these tensors:

$$\dot{W} = V \dot{\mathbf{L}} : \sigma \quad (17)$$

where $V = \det(\mathbf{h}) = \vec{a}_1 \cdot \vec{a}_2 \times \vec{a}_3$ is the volume of the simulation cell. Inserting the expression of $\dot{\mathbf{L}}$ given by equation (10) in (17), and given the symmetry of the stress tensor, we get

$$\dot{W} = \dot{\mathbf{h}} : V \mathbf{h}^{-1} \sigma \quad (18)$$

This relation shows that $V \mathbf{h}^{-1} \sigma$ is the conjugate variable of $\dot{\mathbf{h}}$. Hence, according to the definition (16), the generalized force is identified with

$$F_{(h_{kl})} = V (\mathbf{h}^{-1} \sigma)_{kl} \quad (19)$$

and the equation of motion of \mathbf{h} becomes

$$m_h \ddot{\mathbf{h}} = V \mathbf{h}^{-1} \sigma \quad (20)$$

Like the strain tensor, the stress tensor σ is uniform and periodic. In the same way as the matrix \mathbf{h} replaces the wall degrees of freedom, the tensor σ plays the same role as the force resultants on the walls. It is the sum of two terms: an external stress σ^{ext} applied from outside the system and an internal stress σ^{int} resulting from internal forces:

$$\sigma = \sigma^{\text{int}} + \sigma^{\text{ext}} \quad (21)$$

With periodic boundary conditions, the internal stress tensor σ^{int} should be expressed from contact forces \vec{f} and non-affine velocities \vec{v} of the particles in the simulation cell Ω . It is given by Savage and Jeffrey [1981], Goddard et al. [1995], Bagi [1999]:

$$\sigma^{\text{int}} = n_c \langle \ell \otimes \mathbf{f} \rangle_c + n_p \langle m \mathbf{v} \otimes \mathbf{v} \rangle_p \quad (22)$$

where n_c is the number density of contacts (number of contacts per unit volume), n_p is the number density of the particles, m is the particle mass, and $\vec{\ell}$ is the branch vector (joining the centers of two particles in contacts) The

symbol \otimes denotes the dyadic product. Written in terms of components, we have

$$\sigma_{kl}^{int} = \frac{1}{V} \left\{ \sum_{\alpha=1}^{N_c} \ell_l(\alpha) f_k(\alpha) + \sum_{i=1}^{N_p} m(i) v_k(i) v_l(i) \right\} \quad (23)$$

where N_c and N_p are the numbers of contacts and particles, respectively.

The first average in the expression (22) runs over all contacts α inside the cell. It corresponds to the stresses of static origin related to mechanical equilibrium of particles under the action of contact forces and moments. The second average runs over all particles i in the cell. This term is simply the expression of the kinetic stress resulting from the momenta transported by the particles. It should be remarked that the kinetic energy and stresses involve the non-affine velocities \vec{v} , which represent the particle velocities with respect to the average velocity $\langle \dot{\vec{r}} \rangle = \langle \vec{u} \rangle = \langle \dot{\mathbf{h}} \rangle \vec{s}$. The affine velocities are involved in the advection of particles and play no role in the internal dynamics of the system.

The equation of dynamics for \mathbf{h} takes finally the following form:

$$m_h \ddot{\mathbf{h}} = V \mathbf{h}^{-1} (\sigma^{int} + \sigma^{ext}) \quad (24)$$

with the expression of σ^{int} given by equation (22). Any desired mixed boundary conditions can be applied through this equation to the simulation cell. For example, for triaxial compression in the direction 3, we impose the components $\sigma_{11}^{ext} = \sigma_{22}^{ext}$, the velocity \dot{h}_{33} and the off-diagonal terms $\dot{h}_{kl} = 0$ for $i \neq j$. According to equation (24), the resolution of the equations of dynamics yields $\sigma_{33}^{ext} = -\sigma_{33}^{int}$, $\sigma_{ij}^{ext} = -\sigma_{ij}^{int}$ for the off-diagonal terms, as well as h_{11} and h_{22} as a function of time. It is also possible to impose the invariants of the stress or strain tensors in all space directions by combining the equations of motion for different elements of \mathbf{h} from equation (24) Radjai and Roux [2004].

3.2 Particle degrees of freedom

The Galilean invariance of a periodic system implies that the force resultants $\vec{F}(i)$ acting on the particles are strictly periodic and independent of affine velocities $\vec{u} = \dot{\mathbf{h}} \vec{s}$. For this reason, stress gradients induced by the gravity or other bulk forces can not be introduced in this approach. The conjugate generalized velocities are thus the no-affine velocities $\vec{v}(i)$ of the particles and the power produced by the force $\vec{F}(i)$ is given by $\dot{W}(i) = \vec{F}(i) \cdot \vec{v}(i)$.

The equation of motion describes the motion of a particle following its trajectory. This means that, as for a fluid particle, the velocity changes should be

described by the so-called particulate or Lagrangian derivative. The particulate derivative $D\vec{v}/Dt$ of the non-affine velocity $\vec{v}(i)$ is the sum of a “local” derivative $\partial\vec{v}/\partial t$ of the velocity (at a given point $\vec{r}(i)$ of space) and an “advective” variation $(\vec{v} \cdot \nabla)\vec{u}$ due to the space deformation:

$$\vec{F}(i) = m(i) \frac{D\vec{v}}{Dt} = m(i) \frac{\partial\vec{v}(i)}{\partial t} + m(i) [\vec{v}(i) \cdot \nabla] \vec{u}(i) \quad (25)$$

Remarking that, according to (9), $\vec{u} = \dot{\mathbf{h}} \vec{s} = \dot{\mathbf{h}} \mathbf{h}^{-1} \vec{r} = \dot{\mathbf{L}} \vec{r}$ and setting $\dot{\vec{v}} = \partial\vec{v}/\partial t$, the equation of motion (25) is simply written

$$\vec{F}(i) = m(i) \dot{\vec{v}}(i) + m(i) \dot{\mathbf{L}} \vec{r}(i) \quad (26)$$

Given (2), the equation of motion can also be expressed in the following form:

$$\vec{F}(i) = m(i) \ddot{\vec{r}}(i) - m(i) \ddot{\mathbf{h}} \vec{s}(i) \quad (27)$$

This is a rather intuitive expression as it involves explicitly the acceleration term $m(i) \ddot{\mathbf{h}} \vec{s}(i)$ resulting from the collective degrees of freedom as an inertial force acting on the particle. Combining with equation (24) for \mathbf{h} , we get yet another writing of the equations of motion which does not refer to the reduced coordinates:

$$\ddot{\vec{r}}(i) = \frac{1}{m(i)} \vec{F}(i) + \frac{1}{m_h} V \mathbf{h}^{-1} (\sigma^{int} + \sigma^{ext}) \mathbf{h}^{-1} \vec{r}(i) \quad (28)$$

As we shall see below, this is a convenient representation for an implicit integration scheme. It shows the coupling between the absolute degrees of freedom $\vec{r}(i)$ of the particles and the collective degrees of freedom via the second term which is proportional to the stress and depends on \mathbf{h} . We also note that the product $V (\sigma^{int} + \sigma^{ext})$ does not depend on \mathbf{h} .

Since the periodic deformations of the system depend only on the particle centers, the equations of dynamics for particles rotations are not affected by periodic boundary conditions. The rotations $\vec{\omega}(i)$ of the particles are thus periodic and fully disconnected from the collective degrees of freedom. They are governed by the usual equations of dynamics:

$$\vec{\tau}(i) = \mathbf{I}(i) \dot{\vec{\omega}}(i) + \vec{\omega}(i) \times \mathbf{I}(i) \vec{\omega}(i) \quad (29)$$

where $\vec{\tau}(i)$ is the resultant of force moments and torques acting on the particle i , and \mathbf{I} is the moments of inertia matrix.

The mass m_h attributed to the collective degrees of freedom in equation (28) is an unphysical parameter. It can be compared to the wall masses when the boundary conditions are walls or similar structures such as clumps of particles. Since we want the dynamics to represent that of a large system, the second term of the right-hand side of equation (28) should be small compared to the first term which describes the dynamics of the particles under the action of contact forces. This means that m_h should be large with respect to $m(i)$. In particular, the relaxation time τ towards mechanical equilibrium is proportional to the square root of the mass. Hence, if for the investigation of rheology we search for a well-resolved dynamics of the particles, the collective relaxation time controlled by m_h should be larger than the relaxation time of each particle controlled by its mass $m(i)$ Agnolin and Roux [2007a,b].

4 Integration schemes

The equations to be solved are those of individual particles together with those governing collective degrees of freedom. The integration scheme depends on the numerical method and its variants. We briefly present in this section two schemes for the two methods of contact dynamics and molecular dynamics, respectively.

4.1 Contact dynamics

For the contact dynamics method, it is convenient to use the writings (28) and (24) of the equations of motion. All the positions \vec{r} , \vec{s} and \mathbf{h} are treated explicitly, i.e. fixed during a time step, whereas the velocities $\dot{\vec{r}}$, $\dot{\vec{s}}$ and $\dot{\mathbf{h}}$, the contact forces \vec{f}^α and the non-imposed elements of the tensor of internal moments $\mathbf{M} \equiv V\sigma$ are determined through an iterative scheme. The discretized form of the equations of motion over one time step $[t, t + \delta t]$ is the following:

$$\begin{aligned} \dot{r}_k(i)[t + \delta t] = & \frac{1}{m(i)} \delta t F_k(i)[t + \delta t] + \frac{1}{m_h} \delta t P_{kl}^{int}[t + \delta t] r_l(i)[t] \\ & + B_k(i)[t] \end{aligned} \quad (30)$$

$$\dot{h}_{kl}[t + \delta t] = \frac{1}{m_h} \delta t h_{km}^{-1}[t] M_{ml}^{int}[t + \delta t] + \dot{h}_{kl}[t] \quad (31)$$

$$\begin{aligned} \omega_k(i)[t + \delta t] = & \omega_k[t] + \delta t (I^{-1})_{kl}(i) \tau_l(i)[t + \delta t] \\ & - (I^{-1})_{kl}(i) (\vec{\omega}(i)[t] \times \mathbf{I}(i) \vec{\omega}(i)[t])_l \end{aligned} \quad (32)$$

with

$$M_{kl}^{int}[t + \delta t] = \sum_{\alpha=1}^{N_c} f_k(\alpha)[t + \delta t] \ell_l(\alpha)[t] + \sum_{j=1}^{N_p} m(j) v_k(j)[t] v_l(j)[t] \quad (33)$$

$$P_{kl}^{int}[t + \delta t] = h_{km}^{-1} M_{mn}^{int}[t + \delta t] h_{nl}^{-1} \quad (34)$$

$$P_{kl}^{ext}[t + \delta t] = h_{km}^{-1} M_{mn}^{ext}[t + \delta t] h_{nl}^{-1} \quad (35)$$

$$B_k(i)[t] = \frac{1}{m_h} \delta t P_{kl}^{ext}[t] r_l(i)[t] + \dot{r}_k(i)[t] \quad (36)$$

where the Einstein convention for repeated symbols is assumed. Note that in this scheme the kinetic term in the expression of \mathbf{M}^{int} and the nonlinear term of rotations are treated explicitly.

In the contact dynamics method, the equations of dynamics are expressed (condensed) in the contact frames. The complementarity relations expressing Signorini's condition (between the relative normal velocity and normal force) and Coulomb's law of friction (between the relative tangential velocity at contact and the friction force) are also written in the contact frames Moreau [1994], Jean [1995], Radjai and Richefeu [2009]. With periodic boundary conditions, starting with equations (30) and (32), and iteration loop can be formed for the simultaneous of forces and velocities. During this iterative process, the internal moments tensor \mathbf{M} is updated together with contact forces (the kinetic term kept constant during iterations). The only difference with the usual equations of dynamics lies in the treatment of the term involving internal moments, which controls the propagation of information via the collective degrees of freedom.

The iterative determination of contact forces $\vec{f}^\alpha[t + \delta t]$ and internal moment tensor $M_{kl}^{int}[t + \delta t]$ allows the calculation of velocities $\dot{r}_k(i)[t + \delta t]$, $\omega_k(i)[t + \delta t]$ and $\dot{h}_{kl}[t + \delta t]$ with the help of the discretized equations of motion (30), (31) and (32). The positions are updated from the velocities:

$$h_{kl}[t + \delta t] = h_{kl}[t] + \delta t \dot{h}_{kl}[t + \delta t] \quad (37)$$

$$r_k(i)[t + \delta t] = r_k(i)[t] + \delta t \dot{r}_k(i)[t + \delta t] \quad (38)$$

$$\theta_k(i)[t + \delta t] = \theta_k(i)[t] + \delta t \omega_k(i)[t + \delta t] \quad (39)$$

For the management of periodic boundaries, we need to update the reduced positions and velocities according to the same implicit scheme:

$$\dot{s}_k(i)[t + \delta t] = (h^{-1})_{kl}[t] \{ \dot{r}_l(i)[t + \delta t] - \dot{h}_{kl}[t + \delta t] s_l(i)[t] \} \quad (40)$$

$$s_k(i)[t + \delta t] = s_k(i)[t] + \delta t \dot{s}_k(i)[t + \delta t] \quad (41)$$

4.2 Molecular dynamics

The implementation of periodic boundary conditions in molecular dynamics is rather straightforward. The equations of motion for the collective degrees of freedom are treated like those of individual particles Allen and Tildesley [1987], Peyneau and Roux [2008b], Agnolin and Roux [2007a]. For instance, consider a Gear predictor-corrector scheme of order 3. The positions, velocities and accelerations predicted for the free degrees of freedom are given by a Talor expansion of order 3:

$$r_k^{(p)}(i)[t + \delta t] = r_k(i)[t] + \delta t \dot{r}_k(i)[t] + \frac{1}{2} \delta t^2 \ddot{r}_k(i)[t] \quad (42)$$

$$\dot{r}_k^{(p)}(i)[t + \delta t] = \dot{r}_k(i)[t] + \delta t \ddot{r}_k(i)[t] \quad (43)$$

$$\ddot{r}_k^{(p)}(i)[t + \delta t] = \ddot{r}_k(i)[t] \quad (44)$$

In a similar vein, the collective degrees of freedom are expanded:

$$h_{kl}^{(p)}[t + \delta t] = h_{kl}[t] + \delta t \dot{h}_{kl}[t] + \frac{1}{2} \delta t^2 \ddot{h}_{kl}[t] \quad (45)$$

$$\dot{h}_{kl}^{(p)}[t + \delta t] = \dot{h}_{kl}[t] + \delta t \ddot{h}_{kl}[t] \quad (46)$$

$$\ddot{h}_{kl}^{(p)}[t + \delta t] = \ddot{h}_{kl}[t] \quad (47)$$

The angular degrees of freedom are expanded in the same way:

$$\theta_k^{(p)}(i)[t + \delta t] = \theta_k(i)[t] + \delta t \omega_k(i)[t] + \frac{1}{2} \delta t^2 \dot{\omega}_k(i)[t] \quad (48)$$

$$\omega_k^{(p)}(i)[t + \delta t] = \omega_k(i)[t] + \delta t \dot{\omega}_k(i)[t] \quad (49)$$

$$\dot{\omega}_k^{(p)}(i)[t + \delta t] = \dot{\omega}_k(i)[t] \quad (50)$$

Given the “predicted” positions and velocities, the force laws are used to calculate the contact forces as well as the internal stress tensor σ^{int} and the resultant forces and torques $\vec{F}(i)$ and $\vec{\tau}(i)$ for the particles. The equations of motion (28), (29) and (24) are then used to calculate the “corrected” accelerations $\ddot{r}_k^{(c)}(i)[t + \delta t]$ and $\ddot{h}_{kl}^{(c)}[t + \delta t]$ which are generally different from the predicted accelerations. This difference is used to correct the velocities:

$$\dot{r}_k^{(c)}(i) = \dot{r}_k^{(p)}(i) + \kappa \delta t \{ \ddot{r}_k^{(c)}(i) - \ddot{r}_k^{(p)}(i) \} \quad (51)$$

$$\omega_k^{(c)}(i) = \omega_k^{(p)}(i) + \kappa \delta t \{ \dot{\omega}_k^{(c)}(i) - \dot{\omega}_k^{(p)}(i) \} \quad (52)$$

$$\dot{h}_{kl}^{(c)} = \dot{h}_{kl}^{(p)} + \kappa \delta t \{ \ddot{h}_{kl}^{(c)} - \ddot{h}_{kl}^{(p)} \} \quad (53)$$

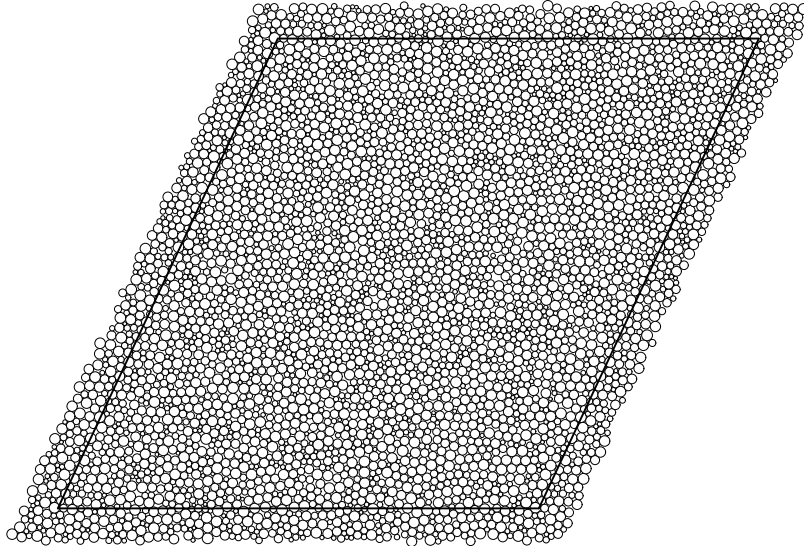


Fig. 3. Example of a system simulated by the molecular dynamics method in 2D. The simulation cell is deformed by simple shear with periodic boundary conditions. The particles in the simulation cell and their images in a thin layer at the interface with neighboring cells are displayed.

where κ is an adjustable coefficient for optimizing the convergence. The new values of the velocities may be used to re-calculate the accelerations from the force laws and this process is repeated until the velocities and accelerations converge within a given precision. The calculated values of the variables are attributed to the end of the time step $t + \delta t$. In this fully explicit scheme, the positions are determined by the expansion according to the equations (42), (45) and (48), and they are therefore not concerned by this iterative process. The positions and velocities of the reduced coordinates are then evaluated from the new values of $\vec{r}(i)$ and \mathbf{h} .

Figure 3 displays an example of a 2D system simulated by the MD method. The simulation cell Ω and particle images in a thin layer are represented. The velocity map is shown in figure 4 for simple shear simulation. The contact interactions lead to a very inhomogeneous field which is periodic in its non-affine part Radjai and Roux [2002]. Figure 5 shows the evolution of packing fraction during a quasi-static cyclic shearing of amplitude $\Delta\varepsilon = 0.04$. The observed gradual compaction of the packing is a well-known property of granular materials.

4.3 Implementation precautions

Some precautions are required for successful simulations with periodic boundary conditions. The round-off numerical errors in collective variables are easily amplified as they are directly reflected by the motions of all particles. For a

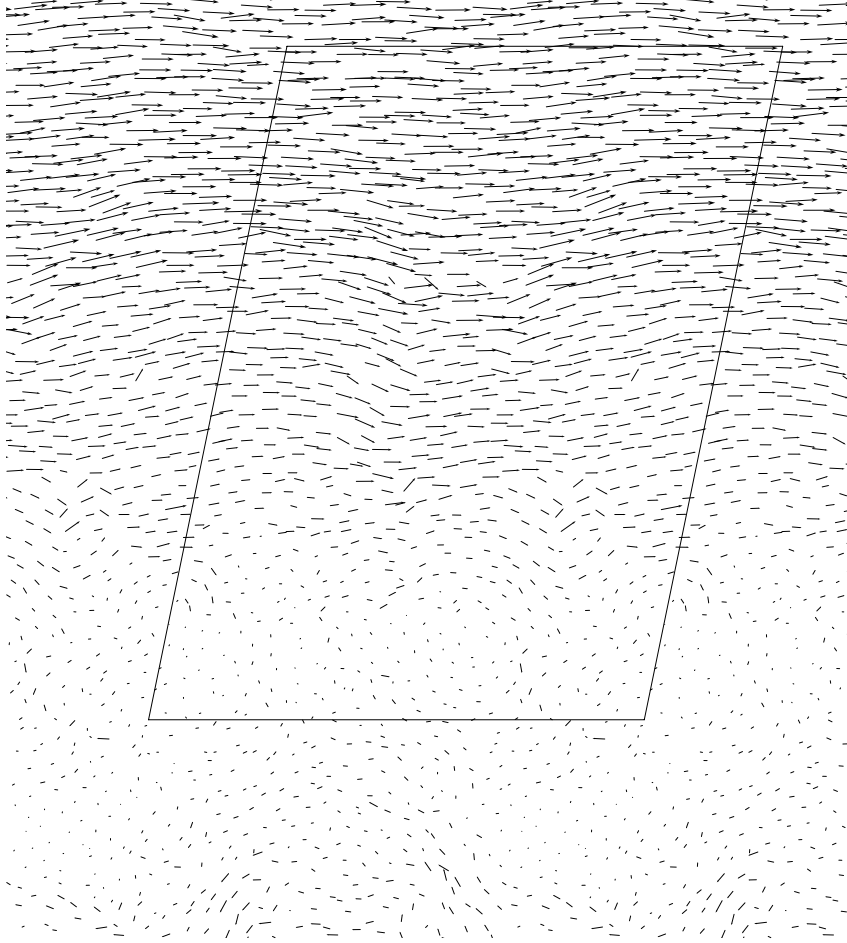


Fig. 4. A map of particle velocities in the simulation cell and neighboring cells under simple shearing with periodic boundary conditions.

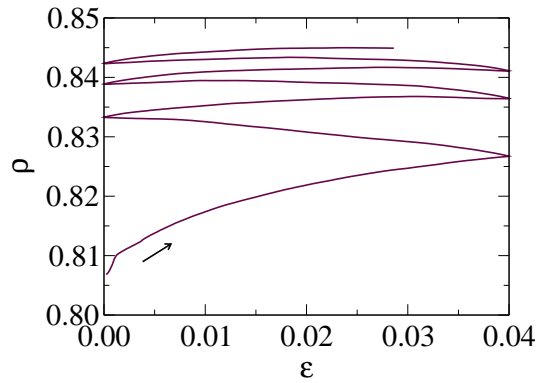


Fig. 5. Evolution of packing fraction during cyclic quasi-static deformation of a sample simulated with periodic boundary conditions.

careful distinction between affine and non-affine velocities, it is important to satisfy the condition $\langle \vec{s} \rangle = 0$ in spite of such round-off errors. For example, the simulation of uni-axial compaction in a given space direction under the action of an applied stress leads to an equilibrium state with $\dot{\mathbf{h}} = 0$ and $\vec{u}(i) = 0$,

but a uniform displacement field $\vec{v}(i) = \mathbf{h} \dot{\vec{s}}(i) \neq 0$. In fact, it can be checked that the equation of motion (26) is compatible with this solution which is a consequence of Galilean invariance of the system of equations. This effect is undesirable for the analysis of the velocity field and it can be avoided by using the comoving reference frame. In practice, it is equivalent to imposing the conditions $\langle \dot{\vec{s}} \rangle = 0$ at every time step when updating the particle positions and velocities.

The same problem is posed with respect to the rigid rotations of the system. In fact, the stress tensor being symmetric, the antisymmetric part of the strain tensor $\dot{\mathbf{L}}$ is immaterial. Therefore, it is necessary to fix three elements of the strain tensor in 3D (one element in 2D). Another possible solution is to cancel the antisymmetric part, which leads in turn to the symmetry of the matrix \mathbf{h} .

5 Conclusion

The numerical simulation of granular materials with periodic boundary conditions is primarily a methodology of producing macroscopically homogeneous strains. This approach eliminates the spurious surface effects resulting from wall boundaries. In some cases, the rigid walls may also be replaced by membrane-like walls and other flexible elements, or by direct application of external forces and displacements on the boundary particles. The method presented here is equivalent to the application of a homogeneous strain (affine field) and the calculation of the deviations from a homogeneous strain for the particles (non-affine field).

The periodic conditions eliminate also any non-periodic internal structure at the scale of the simulation cell. If the typical size of such structures or the correlation length of a microscopic quantity is beyond the linear dimension of the simulation cell, the simulation will be partially influenced by finite size effects. This means that, some particles may interact with their own images. The interactions in granular media are of short range and confined basically to contact interactions. But a granular material involves also mesoscopic structures induced by steric exclusions and rotation frustrations. The force chains and collective particle motions are well-known manifestations of such structures Radjai and Roux [2002]. In the same way, periodic boundary conditions eliminate non-periodic shear bands. Such bands are observed, for instance, orthogonally to the velocity gradient in simple shear Peyneau and Roux [2008b]. But their lifetime is quite short and they disappear upon averaging over a cumulative deformation of 10%.

The implementation of periodic boundary conditions as presented here applies to all space directions. But the same formalism may be applied also in one or

two directions only. For example, a simulation cell may be periodic in the two directions x and y but confined by two parallel walls in the direction z . In this case, the formalism is restricted to the coordinates r_x and r_y of the particles with the corresponding matrix \mathbf{h} and its reduced coordinates. One may then apply either a lateral confining stress or a lateral displacement. The case of lateral imposed displacement is trivial, involving only periodicity in position. This is a particular case of “passive” periodicity. But a general approach, as the one presented in this paper, is required for the application of stresses.

References

- Ivana Agnolin and Jean-Noël Roux. Internal states of model isotropic granular packings. i. assembling process, geometry, and contact networks. *Phys Rev E Stat Nonlin Soft Matter Phys*, 76(6-1):061302, 2007a.
- Ivana Agnolin and Jean-Noël Roux. Internal states of model isotropic granular packings. ii. compression and pressure cycles. *Phys Rev E Stat Nonlin Soft Matter Phys*, 76(6-1):061303, 2007b.
- M. P. Allen and D. J. Tildesley. *Computer Simulation of Liquids*. Oxford University Press, Oxford, 1987.
- K. Bagi. Microstructural stress tensor of granular assemblies with volume forces. *Journal of applied mechanics-Transactions of the ASME*, 66(4):934–936, 1999.
- J. D. Goddard, A. K. Didwania, and X. Zhuang. Computer simulations and experiment on the quasistatic mechanics and transport properties of granular materials. In E. Guazzelli and L. Oger, editors, *Mobile Particulate Systems*, page 261, Dordrecht, 1995. Kluwer Academic Publishers.
- M. Jean. *Frictional contact in rigid or deformable bodies: numerical simulation of geomaterials*, pages 463–486. Elsevier Science Publisher, Amsterdam, 1995.
- J.J. Moreau. Some numerical methods in multibody dynamics: Application to granular materials. *European Journal of Mechanics A/Solids*, supp.(4):93–114, 1994.
- S. Nosé and M.L. Klein. *Mol. Phys.*, 50:1055, 1983.
- S. Nosé and M.L. Klein. Constant-temperature–constant pressure molecular-dynamics calculations for molecular solids: Application to solid nitrogen at high pressure. *Phys. Rev. B*, 33:339–342, 1986.
- M. Parrinello and A. Rahman. Crystal structure and pair potentials: a molecular-dynamics study. *Phys. Rev. Lett.*, 45:1196, 1980.
- Pierre-Emmanuel Peyneau and Jean-Noel Roux. Solidlike behavior and anisotropy in rigid frictionless bead assemblies. *Physical Review E*, 78, 2008a.
- Pierre-Emmanuel Peyneau and Jean-Noel Roux. Frictionless bead packs have macroscopic friction, but no dilatancy. *Physical Review E*, 78, 2008b.

- F. Radjai and V. Richefeu. Contact dynamics as a nonsmooth discrete element method. *Mechanics of Materials*, 41:715–728, 2009.
- F. Radjai and S. Roux. Contact dynamics study of 2d granular media : Critical states and relevant internal variables. In H. Hinrichsen and D. E. Wolf, editors, *The Physics of Granular Media*, pages 165–186, Weinheim, 2004. Wiley-VCH.
- Farhang Radjai and Stéphane Roux. Turbulentlike fluctuations in quasistatic flow of granular media. *Phys Rev Lett*, 89(6):064302, 2002.
- S. B. Savage and D. J. Jeffrey. The stress tensor in a granular flow at high shear rates. *J. Fluid. Mech.*, 110:255, 1981.
- I. Souza and J.L. Martins. Metric tensor as the dynamical variable for variable-cell-shape molecular dynamics. *Phys. Rev. B*, 55:8733–8742, 1997.
- C. Thornton and L. Zhang. A DEM comparison of different shear testing devices. In Y. Kishino, editor, *Powders and grains 2001*, pages 183–190. A.A. Balkema, 2001.